Impact force identification with pseudo-inverse method on a lightweight structure for under-determined, even-determined and over-determined cases

Khoo Shin Yee*[1], Zubaidah Ismail[2], Kong Keen Kuan[1], Ong Zhi Chao[1], Siamak Noroozi[3], Chong Wen Tong[1], Abdul Ghaffar Abdul Rahman[4]

[1]Department of Mechanical Engineering, Engineering Faculty, University of Malaya, 50603 Kuala Lumpur, Malaysia.

[2]Department of Civil Engineering, Engineering Faculty, University of Malaya, 50603 Kuala Lumpur, Malaysia.

[3]School of Design, Engineering & Computing, Bournemouth University, Poole, Dorset, BH12 5BB, UK.

[4]Faculty of Mechanical Engineering, University of Malaysia Pahang, 26600 Pekan, Pahang, Malaysia.

[a]mikeson.khoo@yahoo.com; khooshinyee@um.edu.my, [b]zu_ismail@um.edu.my, [c]keenkuan@yahoo.com, [d]zhichao83@gmail.com, [e]snoroozi@bournemouth.ac.uk, [f]chong_wentong@um.edu.my, [g]dragrahman@yahoo.com

Abstract

Force identification using inverse technique is important especially when direct measurement through force transducer is not possible. Considering the effects of impact excitation force on the integrity of a lightweight structure, impact force identification has become the subject of several studies. A methodology utilising Operating Deflection Shape (ODS) analysis, Frequency Response Function (FRF) measurement and pseudo-inverse method to evaluate the dynamic force is presented. A rectangular plate with four ground supports was used as a test rig to simulate the motions of a simple vehicle body. By using the measured responses at remote points that are away from impact locations and measured FRFs of the test rig, unknown force locations and their time histories can be recovered by the proposed method. The performance of this approach in various

* Corresponding author. Tel: +60162318634; Fax: +6(03)79675317

cases such as under-determined, even-determined and over-determined cases was experimentally demonstrated. Good and bad combinations of response locations were selected based on the condition number of FRF matrix. This force identification method was examined under different response combinations and various numbers of response locations. It shows that in the over-determined case, good combination of response locations (i.e. low average of condition number of FRF matrix) and high number of response locations give the best accuracy of force identification result compared to under-determined and even-determined cases.

Keywords: condition number; frequency response function; impact force identification; pseudo-inverse method; response combination

1. INTRODUCTION

Identification of dynamic force excitation on a system is important for performance evaluation, design optimisation, noise suppression, vibration control as well as condition monitoring. However, there are many situations where the direct measurement of the excitation forces is not possible or feasible. For example, engine torque pulses and shaking forces are difficult to measure since these forces are distributed throughout the engine [1]. In such a case, direct measurement by using force transducer is not possible due to the difficulty of installation and dynamic characteristic altering problem [2]. Therefore, force identification using the inverse method has been developed widely to solve the problem. Much research has been carried out to find the unknown dynamic forces by using the inverse method [3 – 6].

Impact force is the main cause for material fatigue of many structures especially in lightweight structures, so it is useful to understand the characteristics of loading profile, such as impact location and its time history [7]. At the development and modification stage of a lightweight structure design, better information about the loads experienced by the structure through the iteration process will assist the development resulting in a better design. Identification of the input

forces and their locations are helpful to identify areas that are more susceptible to damage. The amplitude of force reflects the vibration condition of the structure so that any requirements for stiffening or structural modification can be identified to preserve a better structural integrity. Once the vibration force can be modelled with practical accuracy, the result can be used as a database for Computer-Aided Engineering (CAE) simulations in trouble-shooting and design improvement analysis for noise and vibration [5]. For example, Hu and Fukunaga [8] developed a Finite Element Method (FEM) model based on the identified force to estimate the various possible internal damages caused by the excitation force. Based on the information of identified forces, real-time health monitoring of a structure is now possible rather than the conventional non-destructive inspection techniques [9, 10] which are not feasible for the on-line operation. Furthermore, identified force is also valuable in other applications. For example, Rahman et al. [11] utilised the identified cyclic loads from ODS of a T-plate structure to determine a suitable excitation level to be used in Impact-Synchronous Modal Analysis (ISMA) [12,13].

The force identification method is used to predict the unknown force from dynamic responses, measured using accelerometers [14] or strain gauges [15]. The measured acceleration responses can be integrated [14] or the measured displacement responses can be differentiated [15] to a form that suits the inverse algorithm. Moreover, the force identification method can be applied for various types of structures, such as beams [14], rods [15] and plates [16]. Many dynamic force identification methods have been developed and a majority of them can be categorised into the direct method and the optimisation method [17].

The direct method identifies excitation force directly by multiplying the system's inverse Frequency Response Function (FRF) with the measured responses. It can be typically classified into two types, i.e. FRF based direct inverse method and Modal Transformation Method (MTM). For example, Hundhausen et al. [18] applied the FRF based direct inverse method to estimate impulsive loads acting on a standoff metallic thermal protection system panel. Hollandsworth and Busby [14] used the MTM to recover the impact force acting on a beam. In general, FRF based direct inverse

78 method has advantages over the MTM in terms of force identification accuracy.

79 The optimisation method finds the unknown input force by matching the estimated and
80 measured responses. For example, Yan and Zhou [19] identified the impact load by using genetic
81 algorithm. Liu and Han [7] conducted a computational inverse procedure to determine the transient
82 loads. Huang et al. [20] applied the optimisation method to identify the impact force from
83 acceleration measurement on a vibratory ball mill. In addition, Sewell et al. [21] presented a
84 development of the artificial neural network difference method to improve accuracy of the Inverse
85 Problem Engine's output. Compared to the direct method, the optimisation method and artificial
86 intelligent method require higher computational and training time.

87 Inversion of transfer function (i.e. Frequency Response Function) matrix that has high
88 condition number and contains measurement errors, will amplify errors in the reconstructed forces.
89 This is known as ill-posed problem. Uhl [22] stated that if a problem of load identification is non-
90 collocated, the ill-posed problem can be encountered. He stated that a non-collocated problem
91 occurs if at least one of the loads does not have a distinguishable influence on any of the sensors.
92 This is typical for many cases, such as a bump-excited impact force, where it is not possible to place
93 accelerometers at the contact points where the loads are generated. Martin and Doyle [23] had
94 clarified some fundamental difficulties and issues involved in this ill-posed problem for the case of
95 impact force identification.

96 Many regularisation methods such as Tikhonov regularisation [24], Singular Value
97 Rejection method [25] and Singular Value Decomposition (SVD) method [26] have been developed
98 to transform the ill-posed problem into a well-posed problem. Liu and Shepard [27] demonstrated
99 that regularisation is only necessary near the structural resonances. On the other hand, Moore-
100 Penrose pseudo-inverse method [28] adopts a least-square solution of the predicted force by
101 forming an over-determined problem, which uses more equations than the number of applied forces
102 to solve the problem. This improves the condition number of the inverse problem, thus reducing the
103 error of identified force to a certain extent.

According to Liu and Han [29], force identification problem can become well-posed once the force location is known in advance. Thus, there are several studies which predict the excitation location prior to predicting the magnitude of the unknown force. For example, Boukria et al. [16] utilised an experimental method based on the minimisation of an objective function created from the transfer functions of several impact locations and measuring points to locate the impact force. Then, the magnitude of the unknown force was identified using Tikhonov method. Briggs and Tse [30] used a pattern matching procedure to identify the location of impact forces on a structure, followed by application of extracted modal constants method to obtain the magnitude of the unknown force. In contrast to the mentioned method, Hundhausen et al. [31] used pseudo-inverse direct method which is able to identify both impact location and magnitude simultaneously. It reduces the computational time and cost. The unknown force locations and their magnitudes can also be adequately identified when the assumed forces are located at where the actual forces act [32].

Instead of utilising the conventional regularisation methods such as Tikhonov method and SVD method to treat the ill-posed FRF matrix, Thite and Thompson [25] proposed an alternative method (i.e. minimum condition number method) to reduce the errors of the identified force. They demonstrated that the selection of response locations with low condition number can reduce the ill-conditioned nature of the FRF. Zheng et al. [33] further improved the method by using coherence analysis, which reduces the computational time and cost. Hence, it is more effective for large-scale models.

In order to reduce the number of sensors used to determine the unknown forces, even-determined case and under-determined case (i.e. number of unknown forces is equal to or greater than the number of equations) cannot be neglected. Furthermore, generation of a robust force identification method for all the three cases (i.e. under-determined, even-determined and over-determined cases) will eventually create a greater competitive advantage to meet customer demands. Previous studies on FRF based direct inverse method and selection of response locations

130 focused on the over-determined case only. The current study initiates an effort to examine the
131 effectiveness of impact force identification via the direct inverse method in all the three cases. In
132 addition, the effect of number of response locations and selection of response locations based on
133 average of condition number are examined for each case.

134 Previous FRF based direct inverse method was mainly applied to collocated cases. In cases
135 where the impact locations are inaccessible, such as bump-excited impact force on a vehicle, a non-
136 collocated force identification method had to be performed by using responses collected at remote
137 points. This current study recommends using responses obtained from remote accelerometers for
138 impact force identification via the pseudo-inverse method. The method uses an algorithm which is
139 able to inverse a non-square matrix. Thus, it is applicable to all the three cases. The performance of
140 this force identification method is experimentally verified for the under-determined, even-
141 determined and over-determined cases.

142 ## 2. THEORY

143 ### *2.1 Frequency Response Function*

144 Frequency Response Function (FRF) is a transfer function that describes the complex relationship
145 between input and output in the frequency domain. It contains the dynamic characteristics of a
146 system, and it is a complex function which is transformable from Cartesian coordinate to polar
147 coordinate and vice versa. FRF only depends on geometric, material and boundary properties of a
148 linear time invariant system, and it is independent of the excitation types. An experimental
149 determination of FRF has the advantage of being applicable to all types of structure and this is
150 useful in structures that have complex boundary conditions. The raw FRF is obtained by use of Eq.
151 (1), which is known as FRF measurement as follows [34]:

152 $$H_{IJ}(\omega)=\frac{CS_{IJ}(\omega)}{AS_{JJ}(\omega)}=\frac{\ddot{X}(\omega)Q^{*}(\omega)}{Q(\omega)Q^{*}(\omega)}\ , \qquad (1)$$

where I and J are output response Degree of Freedom (DOF) and input force DOF respectively. FRF coefficient, H_{IJ} is the ratio of the cross spectrum, CS_{IJ} between input force, Q and output acceleration response, $\ddot{X}$ to the auto spectrum, AS_{JJ} of the input. ω is the angular frequency. $\bullet^*$ is a complex conjugate function.

2.2 Operating Deflection Shape

Operating Deflection Shape (ODS) can be defined as any forced motion of two or more DOFs (points and directions) on a machine or structure [35]. An ODS analysis can animate the vibration pattern of a structure as a function of time or for a specific frequency. For a non-stationary signal such as a transient signal, time-based ODS is extremely useful in giving an overall vibration pattern compared to frequency-based ODS. In this study, time-based ODS is used where all channels of data are acquired simultaneously by using a multi-channel acquisition system. This method is suitable for a small scale test object and it is time efficient.

2.3 The Discrete Fourier Transform

Measured traces in time domain can be transformed into frequency domain or vice versa by using forward and backward Discrete Fourier Transform (DFT) as shown in Eqs. (2) and (3) as follows [36]:

$$F[r] = \frac{1}{BS}\sum_{u=0}^{BS\text{-}1} T[u]e^{-2\pi iru/BS}\Big|_{r=0,1,2,\ldots,BS\text{-}1}, \quad (2)$$

$$T[u] = \sum_{r=0}^{BS\text{-}1} F[r]e^{2\pi iru/BS}\Big|_{u=0,1,2,\ldots,BS\text{-}1}, \quad (3)$$

where $F[r]$ and $T[u]$ are sampled sequences of frequency trace and time trace that have finite length (i.e. non-zero for a finite number of values) at r^{th} sample and u^{th} sample respectively. Block size, BS, is the total number of collected samples. The mathematical operations are evaluated at r = 0, 1,

..., *BS*-1 and *u* = 0, 1, ..., *BS*-1. *i* is equal to $\sqrt{-1}$.

In general, Fast Fourier Transform (FFT) is an efficient algorithm for the computation of the DFT. This is only true if *BS* is a power of two. Their computation speed is obvious when their total number of multiply and add operations are compared, known as $(BS)^2$ for DFT and $(BS)*\log_2(BS)$ for FFT. For example, FFT is 341 times faster than DFT for *BS* that is equal to 4096 samples. In terms of accuracy, both of them produce the same result. Thus, FFT and Inverse Fast Fourier Transform (IFFT) are preferably used in the transformation between frequency and time domains.

2.4 Impact force identification by using pseudo-inverse method

The spatial coordinate equation of motion for forced vibrations of *n* DOF system with viscous damping which describes the test rig under analysis is shown in Eq. (4) as follows:

$$[\mathbf{M}]_{nxn}\{\ddot{\boldsymbol{X}}(t)\}_{nx1}+[\mathbf{C}]_{nxn}\{\dot{\boldsymbol{X}}(t)\}_{nx1}+[\mathbf{S}]_{nxn}\{\boldsymbol{X}(t)\}_{nx1}=\{\boldsymbol{Q}(t)\}_{nx1}, \quad (4)$$

where [M], [C] and [S] are *n* by *n* matrices of mass, damping and stiffness respectively. $\{\ddot{\boldsymbol{X}}(t)\}$, $\{\dot{\boldsymbol{X}}(t)\}$, $\{\boldsymbol{X}(t)\}$ and $\{\boldsymbol{Q}(t)\}$ are *n* by 1 time varying acceleration, velocity, displacement and force vectors respectively. t is time.

The general solution of the linear time invariant vibration system above is expressed in time domain and frequency domain as shown in Eqs. (5) and (6) respectively. The detailed derivation from Eq. (4) to Eqs. (5) and (6) was explained by Wang [17].

$$\ddot{X}(t)=\int_0^t H(t-\tau)Q(\tau)d\tau \ , \quad (5)$$

$$\{\ddot{\boldsymbol{X}}(\omega)\}_{nx1}=[\mathbf{H}(\omega)]_{nxf}\{\boldsymbol{Q}(\omega)\}_{fx1} \ , \quad (6)$$

where $\ddot{X}(t)$ and $Q(\tau)$ are the acceleration response and input force in time domain respectively. $H(t)$ is the impulse response function. t and τ are time. $\{\ddot{\boldsymbol{X}}(\omega)\}$ and $\{\boldsymbol{Q}(\omega)\}$ are *n* by 1

acceleration and force vectors in frequency domain respectively. $[\mathbf{H}(\omega)]$ is a *n* by *f* raw FRF matrix. ω is the angular frequency. *n* and *f* are total number of responses and forces respectively where response DOF, $I = 1, 2, ..., n$ and force DOF, ~~I~~ $J = 1, 2, ..., f$. Note that raw FRF matrix and raw acceleration response are measured by using FRF measurement [34] and time domain ODS analysis [35].

By multiplying pseudo-inverse, *pinv* of measured FRF matrix to measured response vector, the unknown forces can be recovered as shown in Eq. (7). The pseudo-inverse algorithm is shown in Eq. (8).

$$\underset{f\text{x}1}{\{\boldsymbol{Q}(\omega)\}} = pinv\{\underset{n\text{x}f}{[\mathbf{H}(\omega)]}\}\underset{n\text{x}1}{\{\ddot{\boldsymbol{X}}(\omega)\}} \ , \tag{7}$$

$$pinv\{[\mathbf{H}(\omega)]\} = inv\{[\mathbf{H}(\omega)]^{\text{h}}[\mathbf{H}(\omega)]\}[\mathbf{H}(\omega)]^{\text{h}} \ , \tag{8}$$

where *inv* is the direct inverse method. $\bullet^{\text{h}}$ is the complex conjugate transpose of a matrix.

This inverse problem can be categorised into three cases depending on the total number of known responses, *n* and total number of unknown forces, *f*:

(i) Under-determined case: Coefficient *n* is less than coefficient *f*.

(ii) Even-determined case: Coefficient *n* is equal to coefficient *f*.

(iii) Over-determined case: Coefficient *n* is greater than coefficient *f*.

By using pseudo-inverse method, non-collocated (i.e. force and response locations are different) responses are sufficient to identify unknown force. This means that force identification can be done by using remote responses that are a distance away from the impact location. This is illustrated as shown in Eq. (9). Note that force at point 1 can be identified from any responses other than point 1 itself.

$$\begin{Bmatrix} Q_1(\omega) \\ Q_2(\omega) \\ \vdots \\ Q_n(\omega) \end{Bmatrix} = pinv \begin{bmatrix} H_{2:1}(\omega) & H_{2:2}(\omega) & \cdots & H_{2:f}(\omega) \\ H_{3:1}(\omega) & H_{3:2}(\omega) & \cdots & H_{3:f}(\omega) \\ \vdots & \vdots & \ddots & \vdots \\ H_{n:1}(\omega) & H_{n:2}(\omega) & \cdots & H_{n:f}(\omega) \end{bmatrix} \begin{Bmatrix} \ddot{X}_2(\omega) \\ \ddot{X}_3(\omega) \\ \vdots \\ \ddot{X}_n(\omega) \end{Bmatrix} \tag{9}$$

2.5 Selection of response locations based on average of condition number

Different combinations of response locations will have different condition number. In fact, condition number of a matrix measures the sensitivity of the solution of a system of linear equations to errors in the data, and gives an indication of the ill-conditioning of the matrix. Note that condition number near 1 is said to be well-conditioned; condition number far away from 1 is said to be ill-conditioned. The condition number for a square and a non-square matrix can be calculated as follows:

$$CN(\omega) = norm2\{[\underset{nxf}{\mathbf{H}}(\omega)]\} * norm2\{pinv\{[\underset{nxf}{\mathbf{H}}(\omega)]\}\}, \tag{10}$$

where *CN* is the condition number of a FRF matrix. *norm2* is the largest singular value of a matrix.

Average of condition number can be obtained for every combination of response locations as follows:

$$Avg\_CN = \frac{1}{BS}\sum_{r=1}^{BS} CN_r \ , \tag{11}$$

where Avg_CN is the average of condition number. Block size, *BS* is the total number of collected samples. CN_r is the r^{th} sample of calculated condition number where $r = 1, ..., BS$.

3. EXPERIMENTAL SET-UP AND PROCEDURE

3.1 Equipment set-up

The equipment required are a test rig, an impact hammer, 15 accelerometers, a multi-channel data acquisition hardware, a data acquisition software (i.e. DASYLab) and a matrix calculation software (i.e. MATLAB). The experimental set-up for the impact force identification experimental study is shown in Fig. 1.

A test rig was constructed out of a rectangular Perspex plate measuring 20cm in width, 48cm in length, and 0.9cm thick with four ground supports. The plate weighs 1100g. A complex vehicle body inherently comes with infinite DOF. However, it can be simplified into a simple

structure with few DOFs. In this study, the attention is confined to the motion in the vertical plane only. Motions of a vehicle body include rotational (i.e. pitching and rolling modes) and translational (i.e. heaving mode) along the centre of mass of the structure, which usually appear in the low frequency region. In this simple vehicle body simulation, the Perspex plate would produce similar dynamic behaviour as in an actual vehicle body. It contains all the mentioned vibration modes. Thus this simple plate can represent a vehicle body which is generally considered as a lightweight structure. Each of the ground supports is a combination of an aluminium plate and a trapezium steel plate. Dimensions of the aluminium plate are 1.3cm in width, 6.4cm in length, and 8.9cm in height. Detailed dimensions of the steel plate are shown in Fig. 1. The steel plate is made of music wire, which is a high carbon steel with very high yield strength known as spring steel. The thickness of the steel plates near point 1 and point 3 (i.e. 0.2cm) are larger than the plates near point 13 and point 15 (i.e. 0.1cm).

Fifteen accelerometers were attached on the rig and numbered, as shown in Fig. 2. In this study, Wilcoxon Research® Integrated Circuit Piezoelectric (ICP) accelerometer model S100C was used as the response sensor. Considering the accessibility and the flat surface of the test rig, a cyanoacrylate adhesive mount with broad frequency response was chosen. The dimensions of this sensor are 3.73cm in height, 1.98cm in diameter and the weight of the sensor is 45g. The accelerometers are used to measure the responses due to impact force. In this study, Single Input Single Output (SISO) approach or roving accelerometers are not feasible for this test rig as it may cause mass loading effect. Mass loading effect occurs when an additional transducer mass is added to the test rig. This effect would cause data inconsistency throughout the measurement (i.e. shifted FRF). As a rule of thumb, the mass of the accelerometer should be less than one-tenth of the mass of the structure to which it is attached and it also depends on the location of the accelerometer and vibration mode [37]. In this study, 15 accelerometers constitute a significant part of the structure (i.e. 61.36% of the mass of the plate which is 1100g). This affects the dynamic characteristics of the structure. However in the force identification study, Single Input Multiple Output (SIMO) approach

268 is adopted where multiple acceleration responses are measured simultaneously using 11
269 accelerometers. Additional 4 accelerometers at points 1, 3, 13 and 15 were used as dummy masses.
270 All of these 15 accelerometers are assumed to form part of the structure. This ensures the data are
271 collected simultaneously and consistently throughout the measurement. This avoids distortion of
272 FRF due to mass loading effect. In short, the mass loading effect has been eliminated by using the
273 SIMO approach and is suitable for force identification purposes.

274 A modally tuned PCB® ICP impact hammer model 086C03 was used to produce the impact
275 excitation signal. The tip used is medium tip with vinyl cover. In this study, the direction of impact
276 force, *Q* is restricted to the vertical direction and impact location is near to accelerometer at point 13
277 as shown in Fig. 2. By using an impact hammer, the impact force can be measured and recorded,
278 thus providing a means of comparison against the identified impact force from the force
279 identification method.

280 Fig. 1 shows that all of these input force and output response sensors are connected to a
281 multi-channel data acquisition (DAQ) system which consists of four channel DAQ hardware (i.e.
282 model NI-USB 9233) and a compact DAQ chassis (i.e. model NI CDAQ-9172). The DAQ system
283 was connected to a laptop which is equipped with data acquisition software (i.e. DASYLab) and
284 post-processing software (i.e. MATLAB).

285 ***3.2 Procedure***

286 Theoretically, if the FRFs of a linear system and responses caused by excitation forces are known,
287 the unknown force locations and their magnitudes can be calculated by using the inverse FRF
288 technique. This approach is known as FRF based direct inverse method [17]. To identify the
289 unknown forces, a set of digital signal processing procedure is designed and developed as follows:

290 Step (1) - SIMO approach is adopted where 11 multiple acceleration responses are measured
291 simultaneously together with a single reference force. Hence, single column (11 by 1) raw FRF
292 matrix is obtained through FRF measurement as described in section 2.1. A total of 100 averages

are used to reduce the measurement noise. Note that the sampling rate and block size for the signal processing of both FRF measurement and ODS analysis are 2000Hz and 4096 samples respectively. In this study, step (1) is repeated for single reference force acting at points 1, 3, 13 and 15 respectively to obtain an 11 by 4 raw FRF matrix. Then, the measured FRFs are recorded for force identification purposes.

Step (2) - Vibration pattern of a structure can be recorded and visualised when influenced by its excitation force, which is known as ODS analysis as discussed in section 2.2. In this study, an unknown excitation force is excited by an impact hammer at point 13. Force history data is measured by impact hammer for verification purposes. Eleven remote accelerometers are used to measure acceleration time traces at 11 discrete points of the test rig simultaneously once an unknown impact force is applied, to form an 11 by 1 response vector. Next, the acceleration time traces are transformed into frequency domain by using DFT, computed with FFT algorithm as described in Eq. (2).

Step (3) - In this study, the force identification method is tested under three cases: under-determined, even-determined and over-determined cases. In each case, the effect of different combinations of response locations with various averages of condition number is observed and analysed. At the same time, the influence of number of response locations on force identification result is examined in the under-determined and over-determined cases. All corners of the test rig are assumed inaccessible. A single impact force is applied to one of the corners (i.e. point 13) of the test rig and unknown forces for all 4 corners (i.e. points 1, 3, 13, 15) are estimated by using various response combinations as shown in Table 1. The other important experimental parameters such as number of response locations, selection of response locations and average of condition number are also included in Table 1.

Step (4) - The force histories at the 4 corners are identified from non-collocated sensors. By use of Eq. (8), pseudo-inverse method is used to perform the inversion of FRF matrix. After each inversion, the inverted FRF matrix is multiplied with the response vector to identify the unknown

forces for each frequency. After completion of the entire force spectrum, IFFT transforms the identified forces from frequency domain into time domain. Finally, a comparative study between the identified forces and the measured forces are carried out in time domain.

4. RESULTS AND DISCUSSIONS

4.1 Condition number result for all the three cases

The combinations of response locations are selected based on the average of condition number to avoid error amplification due to ill-conditioned problem. In this study, 1, 2, 4, 5 and 11 response locations are chosen from 11 available locations. The total combination of response locations is shown in Table 1. Selecting 5 response locations from 11 available locations would require the most combinations, i.e. 462 combinations. The average of condition number for all the combinations of response locations was calculated by use of Eq. (11). Maximum and minimum averages of the condition number for all possible combinations of response locations, with respect to the number of selected response locations are shown in Fig. 3. These maximum and minimum results are used as a guideline for user to classify the selection of response locations (i.e. good location or bad location). Good location is a combination of response locations with low average of condition number and vice versa. The good and bad locations for the under-determined, even-determined and over-determined cases are selected for further analysis as shown in Table 1.

4.1.1 Condition number result for under-determined case

Fig. 3 shows that one sensor has the lowest average of condition number for both maximum and minimum results. Increasing the number of selected response locations increases both the maximum and minimum results as well as the variation between them. In an under-determined case, there are infinite number of solutions due to number of unknowns outnumber the number of the knowns (i.e. unknown forces to be identified are 4). However, increasing the number of response locations may

improve the solution since it increases the number of known equations to find the unknown forces. The highest average of condition number occurs at the highest number of response locations used in under-determined case, i.e. 3 response locations in this study. Based on the averages of condition number result, lesser sensor is preferred in under-determined case. For the case of 2 sensors, a bad location and a good location are selected for analysis. Another good location from 1 sensor is also selected in this case. Detailed selection of response locations is shown in Table 1. The condition number of selected FRF matrixes in under-determined case is shown in Fig. 4.

4.1.2 Condition number result for even-determined case

As shown in Fig. 3, even-determined case has the highest maximum and minimum averages of condition number and also the highest variation between maximum and minimum result. The maximum value is around 26 times of the minimum value which is the greatest among all cases. Thus, it requires more attention to inverse such a high condition number matrix. In this case, a bad location and a good location are selected for the case of 4 sensors. Detailed selection of response locations is shown in Table 1. The condition number of selected FRF matrixes in even-determined case is shown in Fig. 5.

4.1.3 Condition number result for over-determined case

In Fig. 3, it is found that increasing the level of over-determination reduces the possibility of high condition number while the minimum average of condition number remains the same. Furthermore, increasing the level of over-determination reduces the difference between maximum and minimum averages of condition number. In this study, a bad location and a good location are selected for the case of 5 sensors. Another good location from 11 sensors is also selected for further analysis. Detailed selection of response locations is shown in Table 1. The condition number of selected FRF matrixes in over-determined case is shown in Fig. 6.

4.2 Force identification results for all the three cases

Using Eqs. (7) and (8), different dimensions of FRF matrix can be inversed and hence multiplied with selected combination of response locations in previous section to identify the 4 unknown forces. The force identification results are shown in following section:

4.2.1 Force identification result for under-determined case

For the under-determined case, the identified forces are shown in Fig. 7. All response combinations used are unable to identify the impact location accurately because all 4 locations also show presence of identified forces. Theoretically, only 1 out of the 4 locations should show presence of impact force, where else the rest should remain zero. However, the identified force function acting at point 13 is identical with the measured impact force function. In this case, single response location has the lowest average of condition number (i.e. 1 or well-posed). However, it also has the lowest accuracy of magnitude of impact force compared to the measured force with percentage error of 72.59%. By increasing the number of response locations to 2, force identification result improves. Percentage of errors is reduced to 58.62% and 39.54% for bad and good combinations of response locations respectively. This is because the ratio of known equations to unknown parameters increases and thus, it has approached the exact solution.

The force correlogram between measured force and identified force for selected response locations in under-determined case is shown in Fig. 8. According to Yu and Chan [28], estimated data that falls within ±10% offset from the actual value is considered good and acceptable. Considering the measurement noise effect and error amplification due to ill-conditioned problem especially in the under-determined case, this offset value is adopted in this study. It is set at ±3.5N since the maximum measured force is 33.71N. All estimated data at locations other than point 13 fall outside the offset line, which indicates that the identified impact location by selected response locations is incorrect. Low accuracy in magnitudes of identified force is also obtained for all the

390 combinations of response locations in under-determined case. However, the accuracy of force
391 identification result improves when the number of response locations increases especially when the
392 good location is used.

393 *4.2.2 Force identification result for even-determined case*

394 The identified forces for the even-determined case are shown in Fig. 9. It shows that bad selection
395 of response locations affects the impact force identification result significantly. The result of bad
396 location from 4 sensors shows that magnitudes, functions and locations of identified forces are
397 incorrect and this indicated ill-conditioned problem. Thus, it requires treatment the most (i.e.
398 regularisation method). The force identification result is improved when good location from 4
399 sensors is used. By selecting good location, it is able to find the impact location accurately. The
400 accuracy of force identification result is improved with percentage error of 1.69%. In Fig. 9(c), it is
401 observed that the measured force matches the identified force at point 13 very well especially
402 during impact duration. However, force result outside the impact duration is present as oscillating
403 component due to noise contamination.

404 The force correlogram between measured force and identified force for selected response
405 locations in even-determined case is shown in Fig. 10. It shows that force identification result is
406 inaccurate by using bad location from 4 sensors. This further verified the results observed in Fig. 9.
407 By selecting good location from 4 sensors, the force recovery result has been significantly
408 enhanced. The identified force matches the measured force very well as the estimated data is within
409 the 10% offset.

410 *4.2.3 Force identification result for over-determined case*

411 For the over-determined case, the identified forces are shown in Fig. 11. It is discovered that the
412 force identification result is inaccurate by using bad location from 5 sensors. Furthermore, it is
413 unable to identify the impact location well. The force identification result is improved when good

location from 5 sensors is used. It is able to find the impact location accurately and the accuracy of force's amplitude is good (i.e. percentage of error is 1.60%). By increasing the number of response locations to 11, which has a low average of condition number, it is found that the force identification result is improved slightly (i.e. percentage of error is 1.10%).

The force correlogram between measured force and identified force for selected response locations in over-determined case is shown in Fig. 12. Similar to the even-determined case, it shows unreliable force identification result if bad location is chosen. There is an alternative to improve the force identification result by selecting good location. Result shows that there is a big improvement in identified force result by imposing this method. By increasing the number of response locations, the accuracy of results in this study improves slightly.

4.2.4 Comparison of force identification results by all cases

Combination of results from Figs. 8, 10 and 12 shows that both even-determined and over-determined cases are able to calculate the impact force location well while the under-determined case fails to do so. Combination of results from Figs. 7(c), 9(c) and 11(c) shows that the over-determined case is able to diminish the noise contamination outside the impact duration to a satisfactory level, thus smoothing the identified force. Therefore, there is no oscillating component of identified force found in over-determined case while it is present in both under-determined and even-determined cases. In over-determined case, a least square solution of force identification is obtained to minimise the errors made in every single equation. Therefore, it eliminates the oscillating component.

Combination of results from Figs. 7-12 shows that a good selection of response locations is able to improve the accuracy of force identification result to a satisfactory level for both even-determined and over-determined cases only. However, it shows that good location does not ensure a satisfactory level of force identification result in under-determined case. For example, force identified by good location from 1 sensor has the best average of condition number but it does not

achieve the satisfactory level of force identification result. Meanwhile, bad selection of response locations should be avoided to ensure a reliable force identification result. If this is not the case, special treatment or further signal processing technique such as regularisation method shall be conducted.

The mentioned research outcomes in this paper are summarised in Table 2. By selecting the accuracy result of good location from various sensors, the effect of number of response locations on force identification result is studied, as shown in Fig. 13. It shows that as the number of selected response locations increases, there is improvement in force identification results for under-determined case and over-determined case. Note that this does not apply to even-determined case as the force identification algorithm requires the same amount of responses and unknown forces. Combination of results from Table 2 and Fig. 13 shows that the impact force identification by using pseudo-inverse method is robust and reliable in even-determined and over-determined cases with a priori good selection of response locations.

5. CONCLUSIONS

In this study, impact force identification by using pseudo-inverse method has been examined in three cases: under-determined, even-determined and over-determined cases. Selection of good and bad locations based on the average of condition number is demonstrated. Experimental result shows that the impact force identification by using pseudo-inverse method is robust and reliable in even-determined and over-determined cases when good location can be selected in advance. Force identification using bad location provides unreliable force identification results for all the three cases. Furthermore, increasing number of selected response locations improves the accuracy of force identification result. The pseudo-inverse method is unable to determine the force information accurately in under-determined case even though good sensor configuration is used. Further research shall be conducted to investigate the problem and enhance the accuracy of force identification result to a satisfactory level.

ACKNOWLEDGEMENT

The authors wish to acknowledge the financial support and advice given by Postgraduate Research Fund (PV086-2011A), Advanced Shock and Vibration Research (ASVR) Group of University of Malaya, and other project collaborators. The suggestions and recommendations from reviewers are gratefully acknowledged.

REFERENCES

[1] Starkey J., Merrill G., On the ill-conditioned nature of indirect force-measurement techniques, Journal of Modal Analysis 1989;4:103-108.

[2] Yoon J.-Y., Singh R., Estimation of interfacial forces in a multi-degree of freedom isolation system using a dynamic load sensing mount and quasi-linear models, J. Sound Vib. 2011;330:4429-4446.

[3] Ma C.-K., Lin D.-C., Chang J.-M., Estimation of forces generated by a machine mounted upon isolators under operating conditions, J. Franklin Inst. 1999;336:875-892.

[4] Ma C.-K., Ho C.-C., An inverse method for the estimation of input forces acting on non-linear structural systems, J. Sound Vib. 2004;275:953-971.

[5] Otsuka T., Okada T., Ikeno T., Shiomi K., Okuma M., Force identification of an outboard engine by experimental means of linear structural modelling and equivalent force transformation, J. Sound Vib. 2007;308:541-547.

[6] Yoon J.-Y., Singh R., Indirect measurement of dynamic force transmitted by a nonlinear hydraulic mount under sinusoidal excitation with focus on super-harmonics, J. Sound Vib. 2010;329:5249-5272.

[7] Liu J., Han X., Computational Inverse Procedure for Identification of Structural Dynamic Loads Computational Mechanics, in: Springer Berlin Heidelberg; 2009, p. 323-323.

487 [8] Hu N., Fukunaga H., A new approach for health monitoring of composite structures through
488 identification of impact force, Journal of Advanced Science 2005;17:82-89.
489 [9] Ismail Z., Ibrahim Z., Ong A.Z.C., Rahman A.G.A. Approach to Reduce the Limitations of
490 Modal Identification in Damage Detection Using Limited Field Data for Nondestructive Structural
491 Health Monitoring of a Cable-Stayed Concrete Bridge, J. Bridge Eng. 2012;17(6):867-875.
492 SPECIAL ISSUE: Nondestructive Evaluation and Testing for Bridge Inspection and Evaluation,
493 doi: 10.1061/(ASCE)BE.1943-5592.0000353.
494 [10] Fayyadh M.M., Razak H.A., Ismail Z. Combined modal parameters-based index for damage
495 identification in a beamlike structure: theoretical development and verification, Arch. Civil Mech.
496 Eng. 2011;11(3):587-609.
497 [11] Rahman A.G.A., Ong.Z.C., Z. Ismail, Effectiveness of Impact-Synchronous Time Averaging
498 in determination of dynamic characteristics of a rotor dynamic system, Measurement 2011;44:34-
499 45.
500 [12] Ong. Z.C., Khoo S.Y., Rahman A.G.A., Ismail Z.,Noroozi S., Effect of cyclic force in
501 performing Impact-Synchronous Modal Analysis (ISMA), Journal of Vibration and Acoustic (under
502 review).
503 [13] Rahman A.G.A., Ong Z.C., Ismail Z., Enhancement of coherence functions using time signals
504 in Modal Analysis, Measurement 2011;44:2112-2123.
505 [14] Hollandsworth P.E., Busby H.R., Impact force identification using the general inverse
506 technique, Int. J. Impact Eng. 1989;8:315-322.
507 [15] Ödeen S., Lundberg B., Prediction of impact force by impulse response method, Int. J. Impact
508 Eng. 1991;11:149-158.
509 [16] Boukria Z., Perrotin P., Bennani A., Experimental impact force location and identification
510 using inverse problems: application for a circular plate, Int. J. Mech. 2011;5:48-55.
511 [17] Wang B.T., Prediction of impact and harmonic forces acting on arbitrary structures: theoretical
512 formulation, Mech. Syst. Signal Proc. 2002;16:935-953.

513 [18] Hundhausen R.J., Adams D.E., Derriso M., Kukuchek P., Alloway R., Transient loads
514 identification for a standoff metallic thermal protection system panel, Proc. 23rd Int. Modal Anal.
515 Conf. (IMAC XXIII), Orlando, Florida; 2005.
516 [19] Yan G., Zhou L., Impact load identification of composite structure using genetic algorithms, J.
517 Sound Vib. 2009;319:869-884.
518 [20] Huang H., Pan J., McCormick P.G., Prediction of impact forces in a vibratory ball mill using
519 an inverse technique, Int. J. Impact Eng. 1997;19:117-126.
520 [21] Sewell P., Noroozi S., Vinney J., Amali R., Andrews S., Improvements in the accuracy of an
521 Inverse Problem Engine's output for the prediction of below-knee prosthetic socket interfacial loads,
522 Engineering Applications of Artificial Intelligence 2010;23:1000-1011.
523 [22] Uhl T., The inverse identification problem and its technical application, Archive of Applied
524 Mechanics 2006;77:325-337.
525 [23] Martin M.T., Doyle J.F., Impact force identification from wave propagation responses, Int. J.
526 Impact Eng. 1996;18:65-77.
527 [24] Mao Y.M., Guo X.L., Zhao Y., A state space force identification method based on Markov
528 parameters precise computation and regularization technique, J. Sound Vib. 2010;329:3008-3019.
529 [25] Thite A., Thompson D., Selection of response measurement locations to improve inverse force
530 determination, Appl. Acoust. 2006;67:797-818.
531 [26] Kim S.-J., Lee S.-K., Experimental identification for inverse problem of a mechanical system
532 with a non-minimum phase based on singular value decomposition, Journal of Mechanical Science
533 and Technology 2009;22:1504-1509.
534 [27] Liu Y., Shepard Jr. W.S., Dynamic force identification based on enhanced least squares and
535 total least-squares schemes in the frequency domain, J. Sound Vib. 2005;282:37-60.
536 [28] Yu L., Chan T.H.T., Moving force identification based on the frequency–time domain method,
537 J. Sound Vib. 2003;261:329-349.
538 [29] Liu G.R., Han X., Computational inverse techniques in non-destructive evaluation, CRC; 2003.

[30] Briggs J.C., Tse M-K., Impact force identification using extracted modal parameters and pattern matching, Int. J. Impact Eng. 1992;12:361-372.

[31] Hundhausen R.J., Adams D.E., Derriso M., Impact loads identification in standoff metallic thermal protection system panels. Journal of Intelligent Material Systems and Structures 2007;18 (6):531-541. doi: 10.1177/1045389x06067141.

[32] O'Callahan J., Piergentili F., Force estimation using operational data, in: Proceedings of 8th International Modal Analysis Conference; 1996, p. 1586-1592.

[33] Zheng S., Zhou L., Lian X., Li K., Technical note: Coherence analysis of the transfer function for dynamic force identification. Mechanical Systems and Signal Processing 2011;25(6):2229-2240. doi: 10.1016/j.ymssp.2011.01.015.

[34] Halvorsen W.G., Brown D.L., Impulse technique for structural frequency response testing, J. Sound Vib. 1977;11:8-21.

[35] Schwarz B.J., Richardson M.H., Introduction to operating deflection shapes, CSI Reliability Week, Orlando, FL; 1999.

[36] Soon B.Y., Eloe P.W., Kammler D., The fast Fourier transform method and ill-conditioned matrices, Applied Mathematics and Computation 2001;117(2–3):117-129. doi: 10.1016/s0096-3003(99)00171-x.

[37] Baharin N.H., Rahman R.A., Effect of accelerometer mass on thin plate vibration, Jurnal Mekanikal 2009;29:100-111.

565 **LIST OF FIGURE & TABLE CAPTIONS**

566 **List of Figures**

567

568

List of Tables

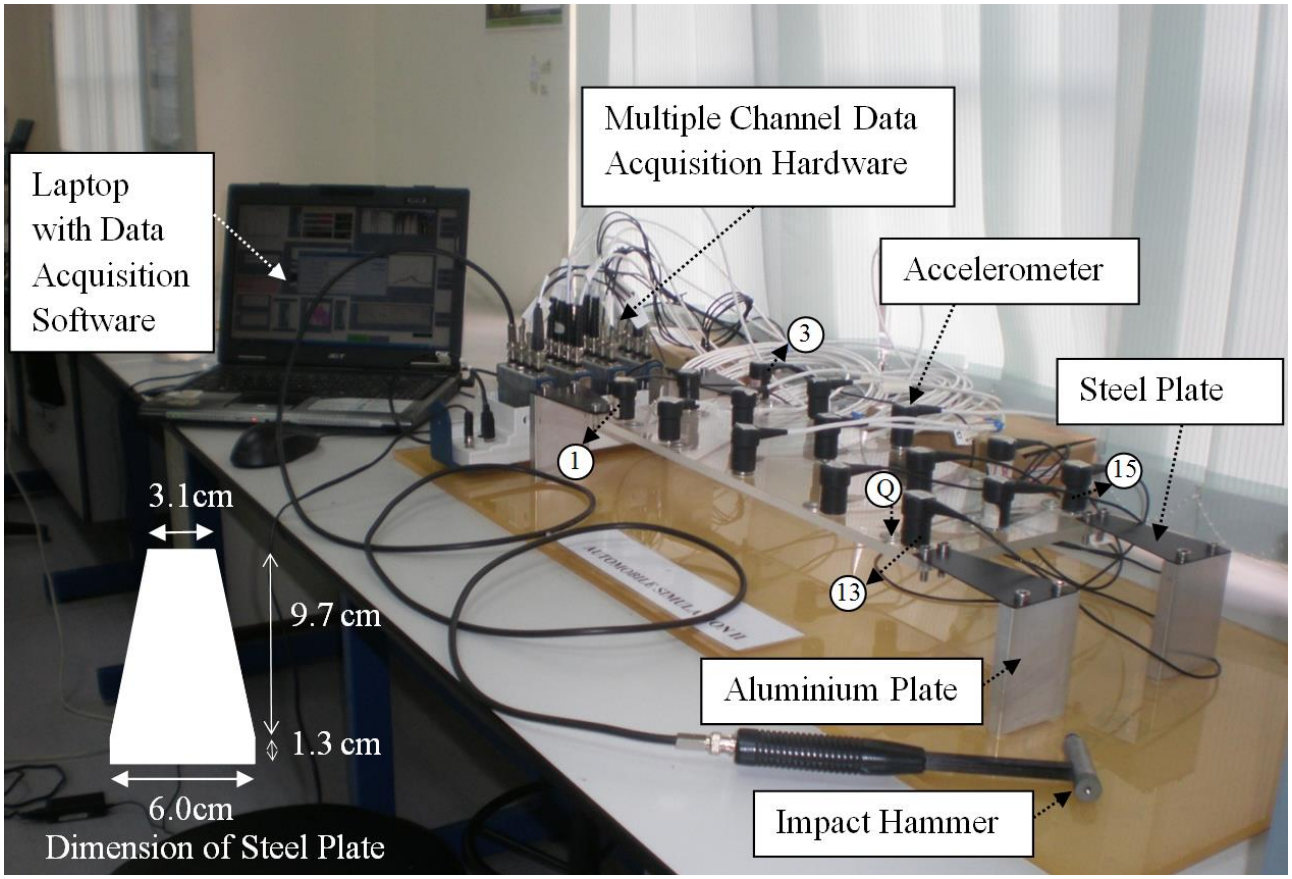

Fig. 1. Experimental set-up for impact force identification experimental study.

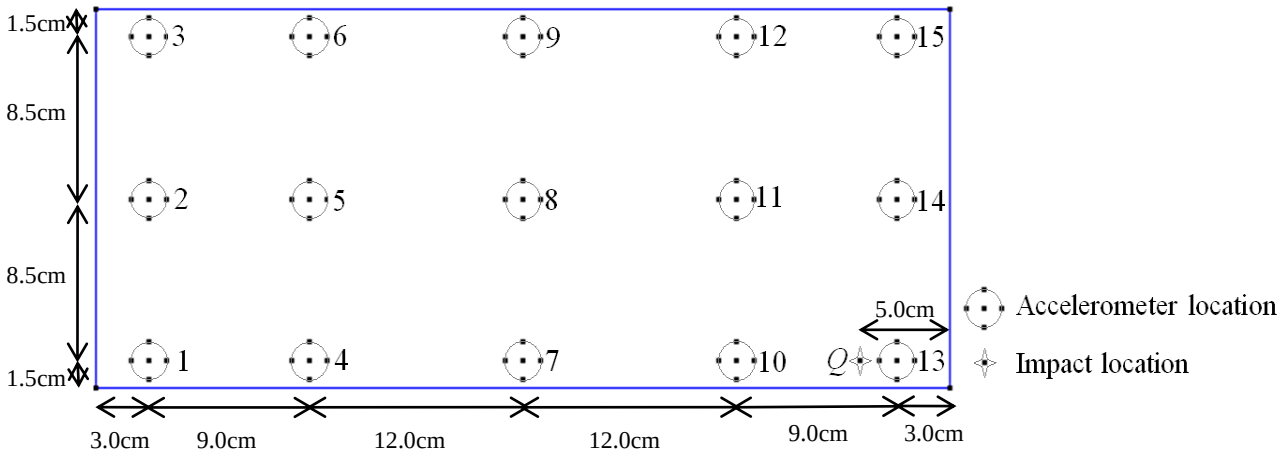

Fig. 2. Schematic drawing of test rig.

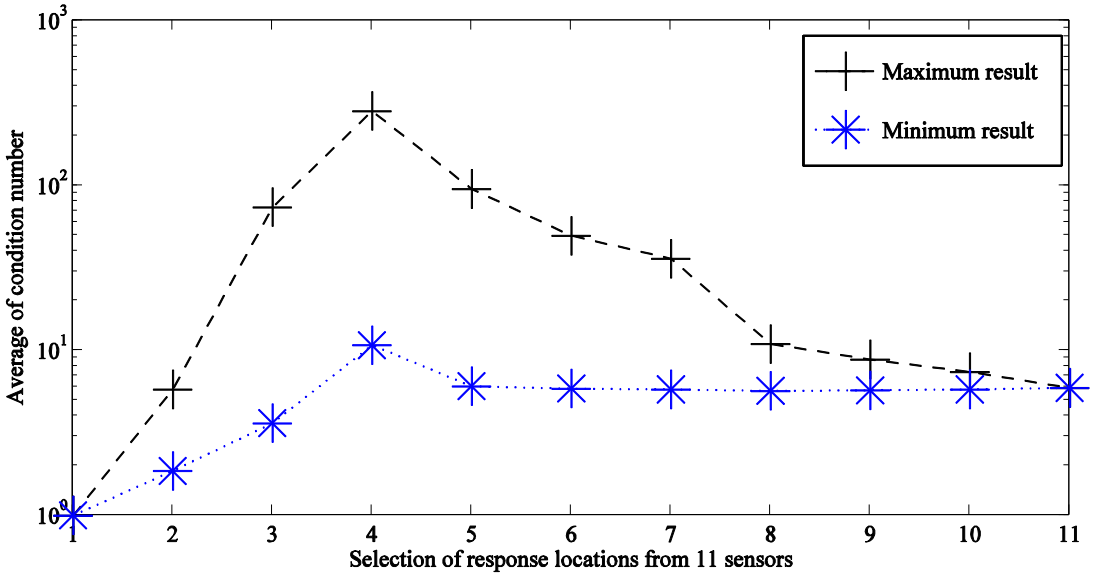

Fig. 3. Graph of average of condition number versus selection of response locations from 11 sensors.

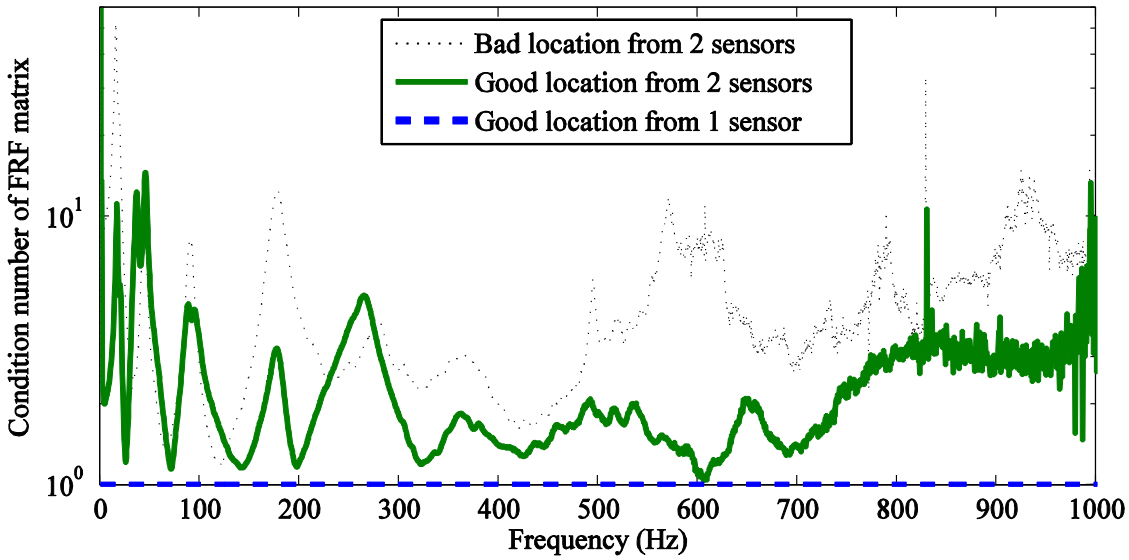

643

644 Fig. 4. Graph of condition number of FRF matrix in frequency domain for under-determined case.

645

646

647

648

649

650

651

652

653

654

655

656

657

658

659

660

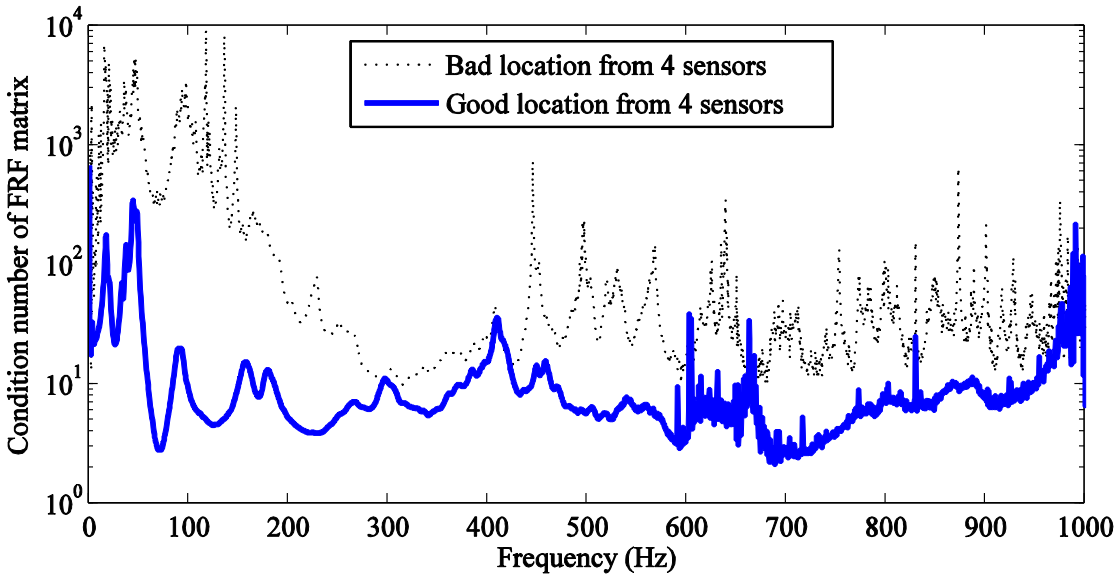

Fig. 5. Graph of condition number of FRF matrix in frequency domain for even-determined case.

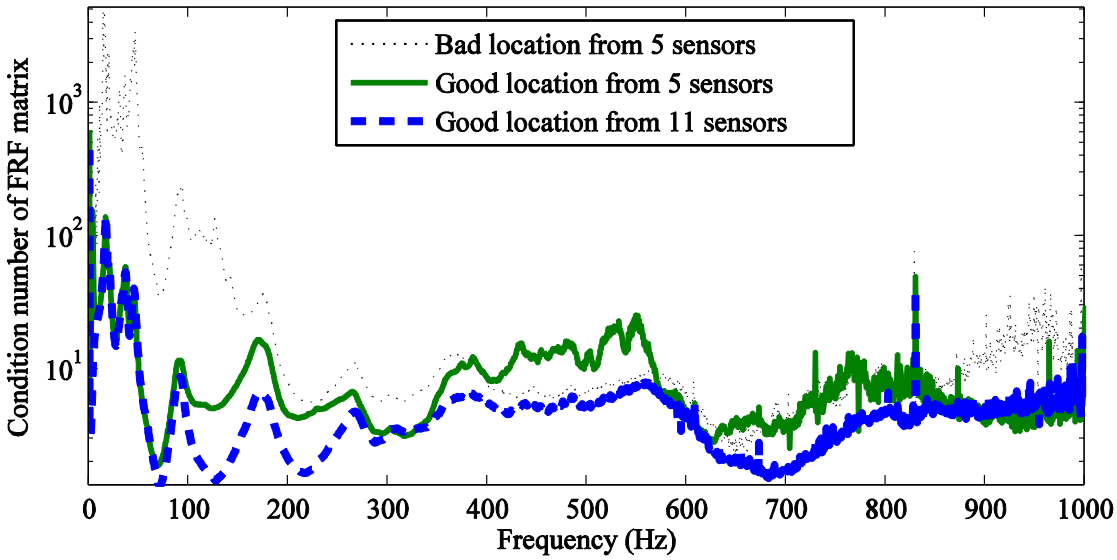

679

680 Fig. 6. Graph of condition number of FRF matrix in frequency domain for over-determined case.

681

682

683

684

685

686

687

688

689

690

691

692

693

694

695

696

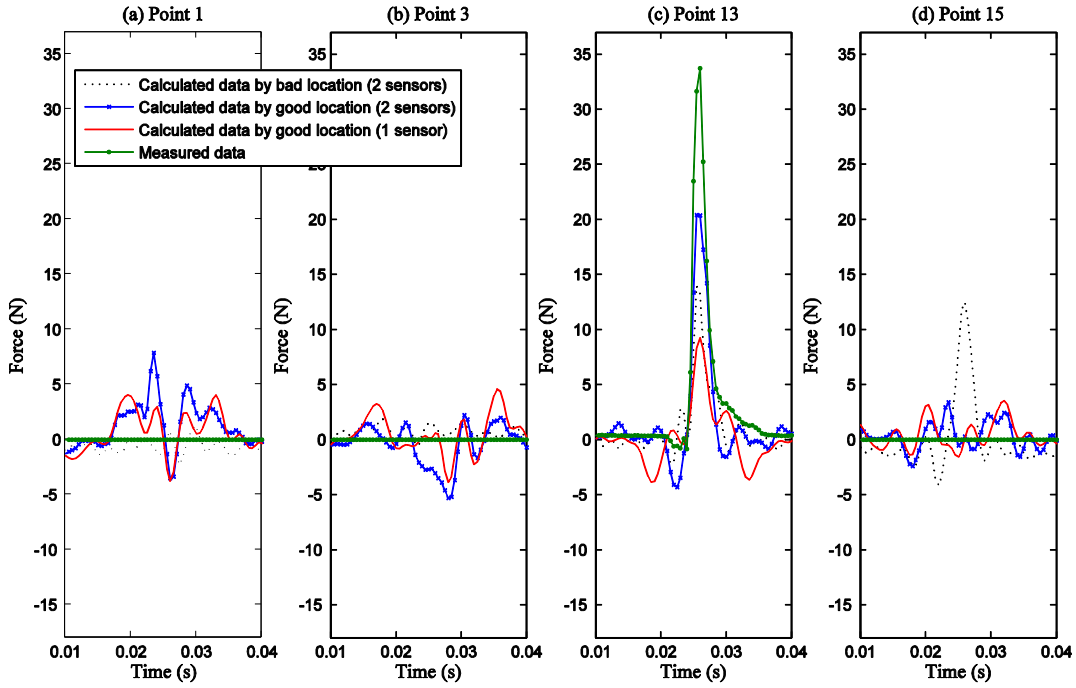

Fig. 7. Comparison of force histories identified from various response combinations in under-determined case at four discrete locations: (a) point 1 (b) point 3 (c) point 13 (d) point 15.

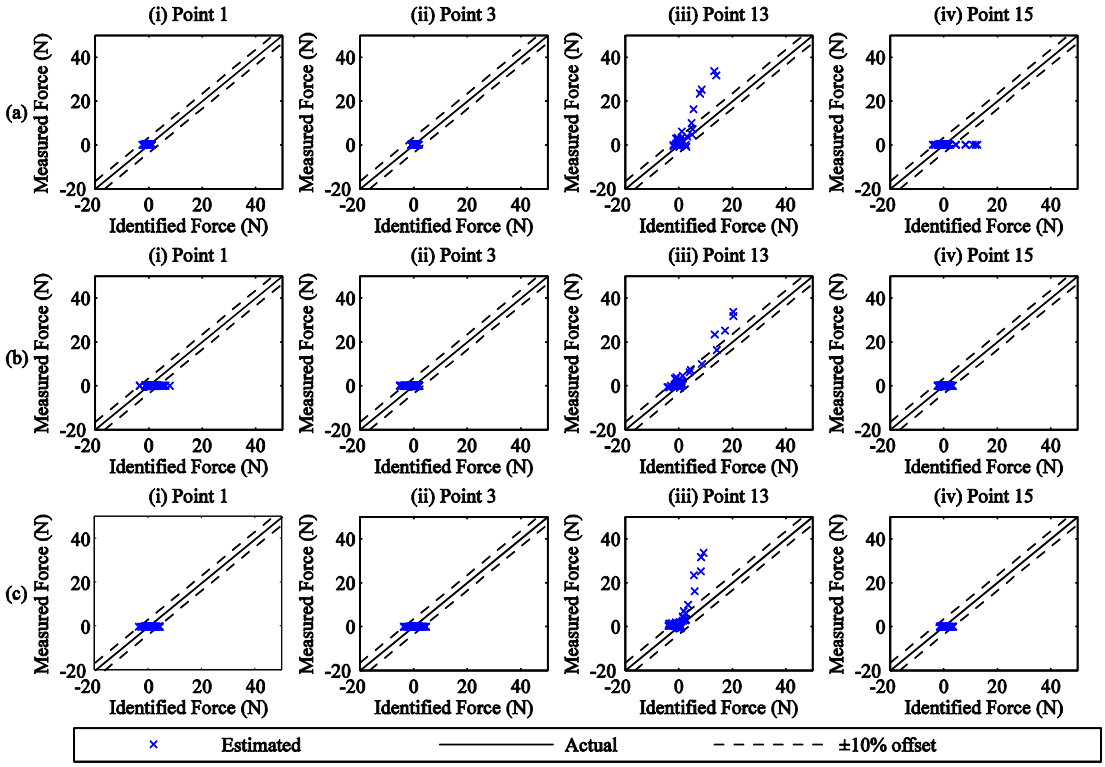

Fig. 8. Force correlogram at four discrete locations for various response combinations in under-determined case: (a) bad location from 2 sensors (b) good location from 2 sensors (c) good location from 1 sensor.

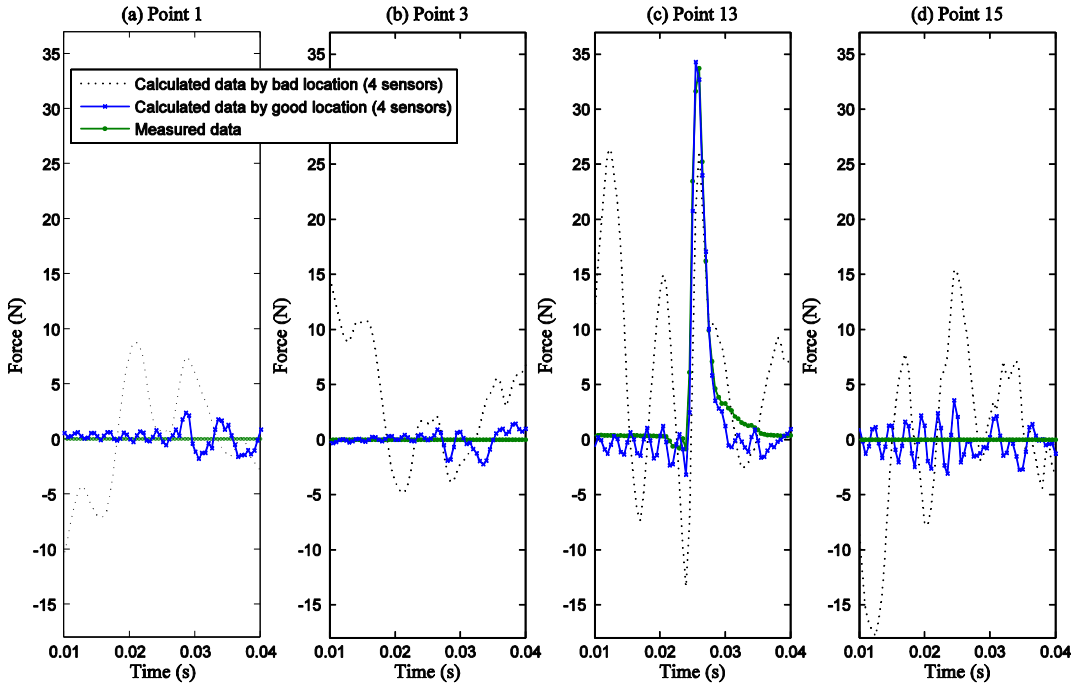

727

728 Fig. 9. Comparison of force histories identified from various response combinations in even-

729 determined case at four discrete locations: (a) point 1 (b) point 3 (c) point 13 (d) point 15.

730

731

732

733

734

735

736

737

738

739

740

741

742

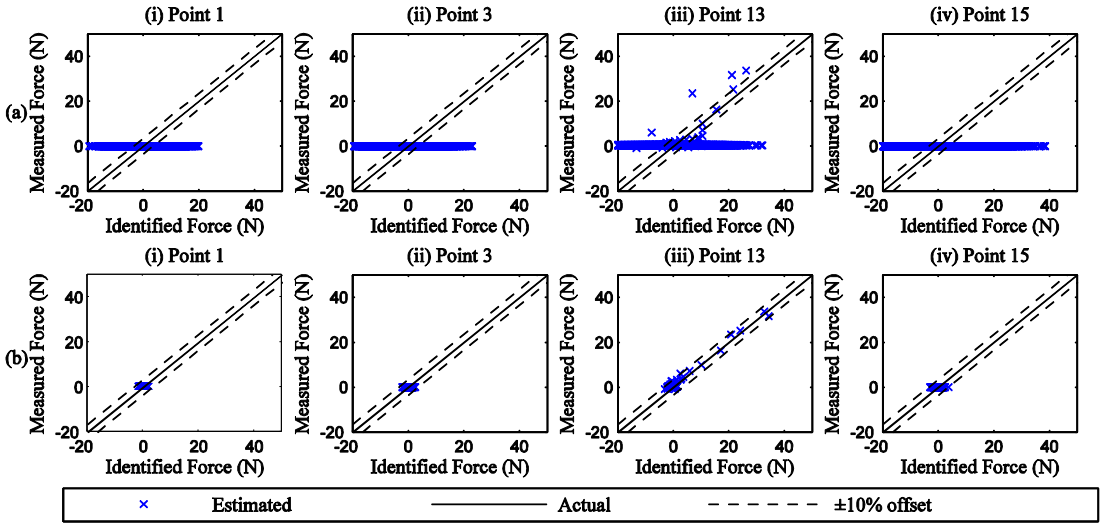

743

744 Fig. 10. Force correlogram at four discrete locations for various response combinations in even-

745 determined case: (a) bad location from 4 sensors (b) good location from 4 sensors.

746

747

748

749

750

751

752

753

754

755

756

757

758

759

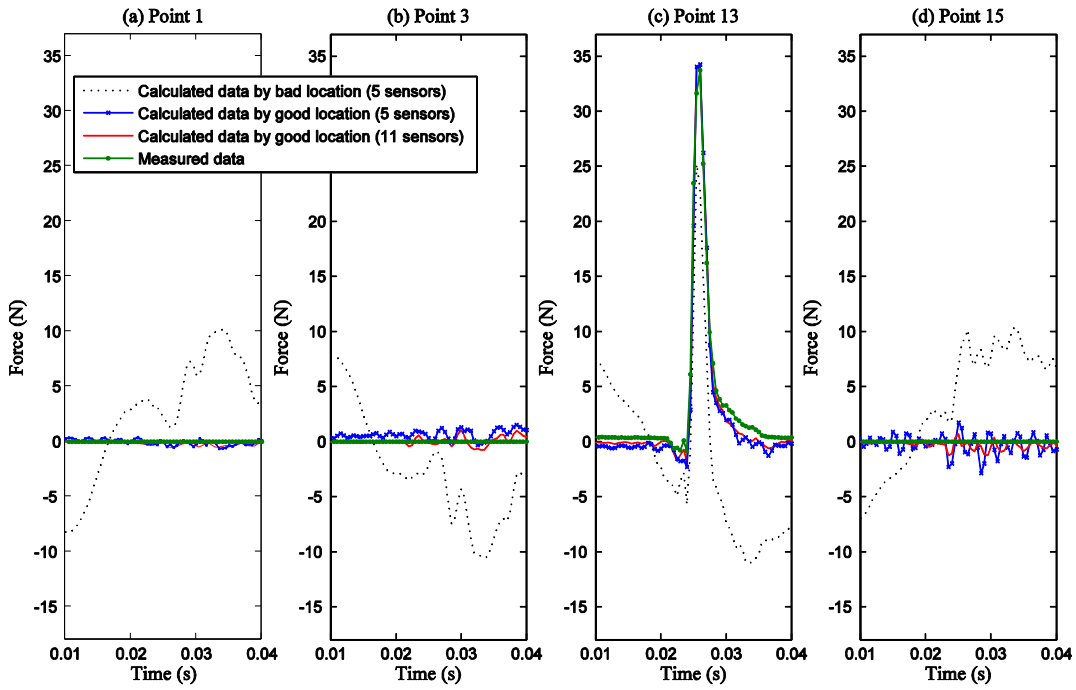

760

761 Fig.11. Comparison of force histories identified from various response combinations in over-

762 determined case at four discrete locations: (a) point 1 (b) point 3 (c) point 13 (d) point 15.

763

764

765

766

767

768

769

770

771

772

773

774

775

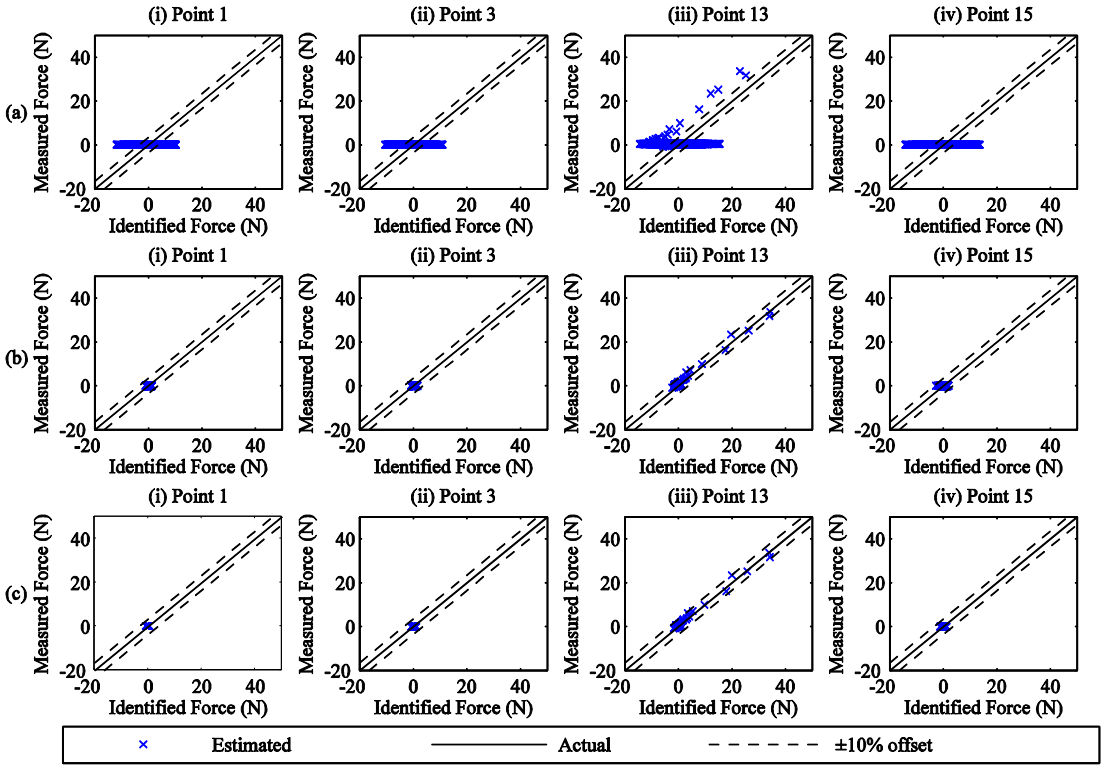

Fig. 12. Force correlogram at four discrete locations for various response combinations in over-determined case: (a) bad location from 5 sensors (b) good location from 5 sensors (c) good location from 11 sensors.

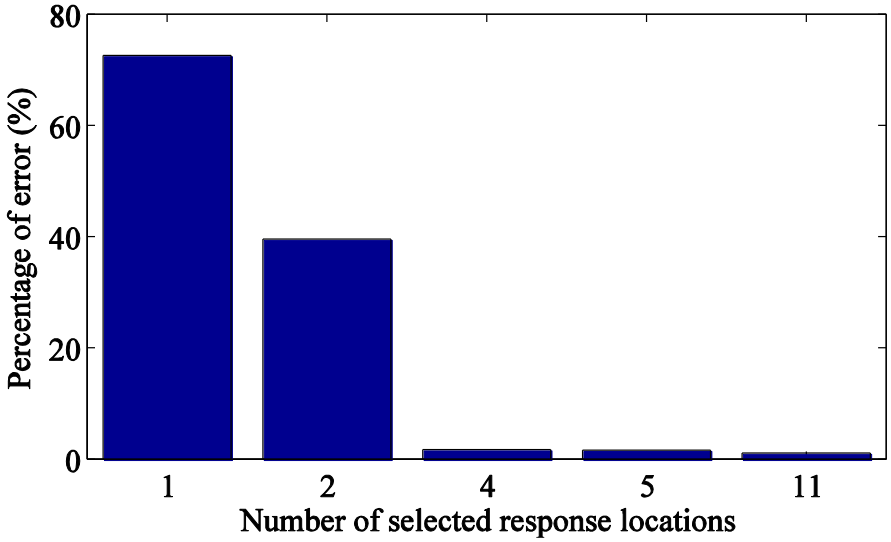

Fig. 13. Graph of percentage of error between measured force and identified force at point 13 versus number of selected response locations.

Table 1. Experimental parameters.

Identified force location	1,3,13,15 (total 4 estimated forces)							
Non-collocated response locations	2,4,5,6,7,8,9,10,11,12,14 (total 11 responses locations)							
Case	Under-determined			Even-determined		Over-determined		
Number of response locations	1	2		4		5		11
Total combination of response locations	11	55		330		462		1
Selection of response locations	6	5,8	6,10	2,4,5,6	2,6,10,14	4,5,6,11,14	5,6,7,10,12	All
Average of condition number	1	4.92	2.47	233.46	13.20	73.48	9.19	5.92
Location classification	Good	Bad	Good	Bad	Good	Bad	Good	Good

826 Table 2. Comparison between force identification results for under-determined, even-determined

827 and over-determined cases.

Category		Identified impact location	Identified function at point 13	Percentage of error (%)
(a) Under-determined case	(i) Bad location (2 sensors)	Point 13 & 15	Impact force with small oscillating component	58.62
	(ii) Good location (2 sensors)	Point 1,3 & 13	Impact force with small oscillating component	39.54 ↓
	(iii) Good location (1 sensor)	Point 1,3 & 13	Impact force with small oscillating component	72.59 ↑
(b) Even-determined case	(i) Bad location (4 sensors)	Point 1,3,13 & 15	Impact force with very large oscillating component	22.31
	(ii) Good location (4 sensors)	Point 13	Impact force with small oscillating component	1.69 ↓
(c) Over-determined case	(i) Bad location (5 sensors)	Point 1,3,13 & 15	Impact force with very large oscillating component	25.30
	(ii) Good location (5 sensors)	Point 13	Impact force without oscillating component	1.60 ↓
	(iii) Good location (11 sensors)	Point 13	Impact force without oscillating component	1.10 ↓

828

829